frontiers | Frontiers in Earth Science

ORIGINAL RESEARCH
published: 08 July 2022
doi: 10.3389/feart.2022.908193

Early Cretaceous Volcanic Edifice Activity in the Sulu Orogenic Belt: Evidences From Volcanic-Sedimentary Rhythm Characteristics in Lingshan Island, Eastern Shandong Province, China

Ruiyang Liu[1,2,3], Yaoqi Zhou[1,2,3], Shihui Dong[1], Tengfei Zhou[1]*, Hongyu Mu[1], Bingyang Bai[1], Sunyi Li[1], Tongtong Chen[1,2,3] and Zhenkai Zhang[1,4]*

[1]School of Geosciences, China University of Petroleum, Qingdao, China, [2]State Key Laboratory of Shale Oil and Gas Enrichment Mechanisms and Effective Development, Beijing, China, [3]Key Laboratory of Petroleum Accumulation Mechanisms, SINOPEC, Wuxi, China, [4]Shaanxi Center of Mineral Geological Survey, Shaanxi Institute of Geological Survey, Xi'an, China

OPEN ACCESS

Edited by:
Hossein Azizi,
University of Kurdistan, Iran

Reviewed by:
Renchao Yang,
Shandong University of Science and Technology, China
Yousif Mohammad,
University of Sulaymaniyah, Iraq

***Correspondence:**
Yaoqi Zhou
zhouyq@upc.edu.cn
Tengfei Zhou
zhoutfgeoscience@126.com

Specialty section:
This article was submitted to Sedimentology, Stratigraphy and Diagenesis, a section of the journal Frontiers in Earth Science

Received: 11 April 2022
Accepted: 26 May 2022
Published: 08 July 2022

Citation:
Liu R, Zhou Y, Dong S, Zhou T, Mu H, Bai B, Li S, Chen T and Zhang Z (2022) Early Cretaceous Volcanic Edifice Activity in the Sulu Orogenic Belt: Evidences From Volcanic-Sedimentary Rhythm Characteristics in Lingshan Island, Eastern Shandong Province, China. Front. Earth Sci. 10:908193. doi: 10.3389/feart.2022.908193

A rhyolitic tuff-mudstone interbedded rock outcrop with a good rhythm is found in the Yangjiaodong area of Lingshan Island, eastern Shandong Province. The volcanic eruption dynamics process was investigated by using the rhythm of volcanic accumulation method. Combined with the geologic setting of the study area, the parameter deposition rate is 6.5 m/Ma, and the mudstone compaction factor is 0.3 because the study area is the Ri-Qing-Wei Basin, which is the volcanic back-arc basin with insufficient source supply. Based on this, the time span of the analyzed sample was calculated to be 2.24 Ma, which represents the duration of this eruption event. We used software called Acycle to finish this research. The result shows cyclicity of 2.296, 5.78, 8.475, and 15.625 kyr and the scales of 2.17, 2.94, 3.12, and 18.87 m repeatability. Considering that magma eruption is affected by changing melt conditions, the crystallinity, water content, temperature, and pressure are comprehensively considered "activation conditions" to predict the dynamic process within the near-surface magma chamber, which is characterized using a pulsed volcanic eruption model.

Keywords: magmatic dynamics, melt evolution, highly differentiated magma, Lingshan Island, volcanic-sedimentary rhythm

1 INTRODUCTION

In recent years, previous studies on magma and magmatic rocks of the Qingshan Group in Lingshan Island have focused on magmatic rock geochemistry, geotectonic, coupling processes of magmatic activity as well as tectonic movement, and magmatic evolution (Zhang et al., 2013; Zhang et al., 2015; Zhou et al., 2015; Liang, 2016; Zhou et al., 2017; Ao et al., 2018; Dong, 2020; Zhou et al., Forthcoming 2022). However, few studies have focused on the high-differential magmatic rocks of the island, and research on the volcanic activity cycle has been limited to the evolutionary sequencing (Zhang, 2017). No qualitative and quantitative studies on the dynamic evolution process of the near-surface magmatic chambers have been conducted. Previous studies have shown that the dynamic evolution process of the magma chamber have a certain rhythm (Hofmann, 2012; Wotzlaw et al., 2022), by

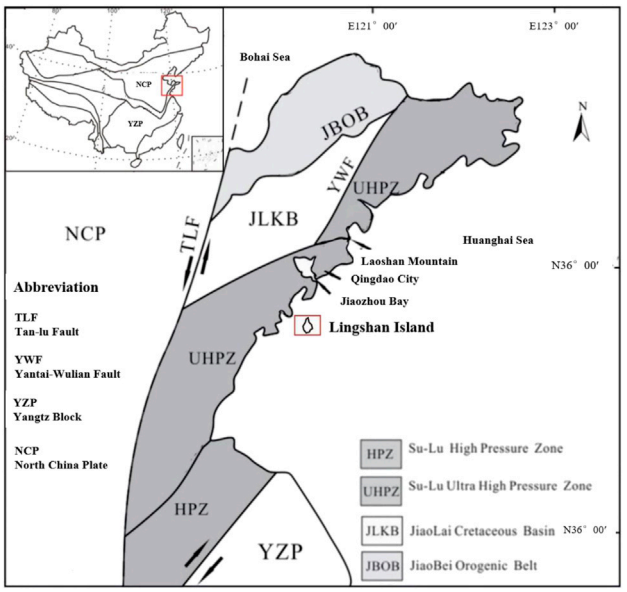

FIGURE 1 | Simplified map of China showing major blocks and its boundaries and geological map of east Shandong.

using time series signal analysis technology to correlate the response of volcanic accumulation rhythm to volcanic eruption dynamics comprehensively.

Acycle software spectrum analysis can be used to quantify disperse geological data (Huang, 2014; Yang et al., 2021). Generally, the volcanic-sedimentary strata exposed on the surface reflect the underground magmatic activity. Time series spectrum analyses of volcanic-sedimentary interbedded rock samples can be performed to summarize the dynamic evolution model of the magma chamber, melting in the upper crust (Annen, et al., 2006; Cooper and Kent, 2014; Bachmann, et al., 2004; Reubi and Blundy, 2009; Karakas et al., 2019; Jackson et al., 2018; Feng et al., 2020; Feng et al., 2021; Wang et al., 2021; Ma and Li, 2017; Doucet et al., 2020; Ma et al., 2020). In this study, the geological characteristics of the region and cycle times and volcanic scale of the Early Cretaceous rhyolitic volcanic magmatic activity on Lingshan Island are identified, providing a knowledge base for the highly differentiated magmatic activity on the island.

2 GEOLOGICAL SETTING

Lingshan Island is located in the Ri-Qing-Wei Basin (Zhou et al., 2015), in the interior of the Sulu orogenic belt (**Figure 1**). The Ri-Qing-Wei Basin is a Late Mesozoic offshore rift basin in eastern Shandong Province, located between Qianliyan Uplift and Jiaonan Uplift. Jiaonan Uplift belongs to the *Sulu* orogenic belt, formed by the collision of the North China Plate and Yangtze Plate in the Triassic. The main fault strikes NE to SW and controls the tectonic unit and the occurrence of depression within the basin (Zhou et al., 2015; Zhang et al., 2015; Zhang, 2017; Liu et al., 2016; Wu et al., 2017). A massive extension occurred in the late Mesozoic, caused by the subduction and retreat of the PaleoPacific Plate and the rollback of the Izenaqi Plate (Zhang et al., 2020; Liu et al., 2020; Zhao et al., 2021). The regional lithosphere has undergone thinning-thermal-upwelling-stretching-detachment (Sun et al., 2018; Wang et al., 2020; Feng et al., 2021), resulting in the development of a large-scale trans-crustal magmatic system (Cashman et al., 2017; Zhou et al., 2018) and acidic magma of Lingshan Island, which originated from the partial melting of the upper crust. Lingshan Island is a single-sided mountain-type island (Meng and Li, 2019), with a NEE-trending syncline through the entire strata assembly. The genesis of Lingshan Island comprises various tectonic and dynamic processes, resulting from lithospheric delamination, mantle diapir-dominated surface extension, and magmatic activity (Liu et al., 2016). The tectonic evolution of the Early Cretaceous experienced the action of extension-extrusion-extension. The white rhyolitic tuff on the island is mainly distributed on the south side, visible in typical sections such as Chuanchang, Laohuzui, and Yangjiaodong. The Yangjiaodong area has an exposed gray–white rhyolite layer up to 15–20-m-thick (Ao et al., 2018), with rhythmic characteristics (**Figure 2A**). It mainly comprises light tuff and dark tuffaceous sedimentary mudstone, indicating that the sedimentation and volcanism on Lingshan Island were synchronized over time (Meng et al., 2018).

The Yangjiaodong area develops a complete volcanic-sedimentary stratum of the Qingshan Group. From bottom to top, volcanic clastic rocks and terrigenous clastic rock deposits, rhyolite, terrigenous clastic rocks with multiple sets of volcanic debris-flow deposits, and volcanic lava layers are developed (Zhou et al., 2017; Zhang et al., 2019). The strata investigated in this study are tuff interbedded in the upper part of the second thick white rhyolite layer, belonging to a volcanic-sedimentary facies (**Figure 2B**). The volcanic-sedimentary rhythms in rhyolite beds are investigated, utilizing the volcanic-sedimentary cycle to describe the dynamics of volcanically erupted magma. Previous geochemical analyses and chronology tests on white rhyolite in the Yangjiaodong area, obtained the following results. Lingshan Island rhyolite is high in silicon and potassium, and low in phosphorus, magnesium, titanium, calcium, and iron (Ao et al., 2018; Dong, 2020). Enrichment of large ion lithophile elements and light rare earth elements, and loss of high field strength elements were noted, resulting in a weakly peraluminous, high potassium calcareous rock series, and typical of acidic volcanic rock (Ao et al., 2018; Meng et al., 2018; Dong, 2020). Typically, a highly differentiated I-type rhyolite (containing common dark mineral phenocrysts such as hornblende and biotite), results from postcollisional magmatism in the Sulu orogenic belt (Wang et al., 2021). The extension of the lithosphere provides a channel for the rise of rhyolite showing in **Figure 10** (Zhou et al., 2018). Locally, rhyolites have a relatively high alkali content because they cannot be formed by direct differentiation of mantle-derived magma, affording speculation that high alkali-felsic magma is primarily caused by partial melting of pure crust-derived materials (Zhang et al., 2019). Major elements in Lingshan Island strata are very large. Trace elements and rare earth elements are characterized by the enrichment of Ba, La, Th,

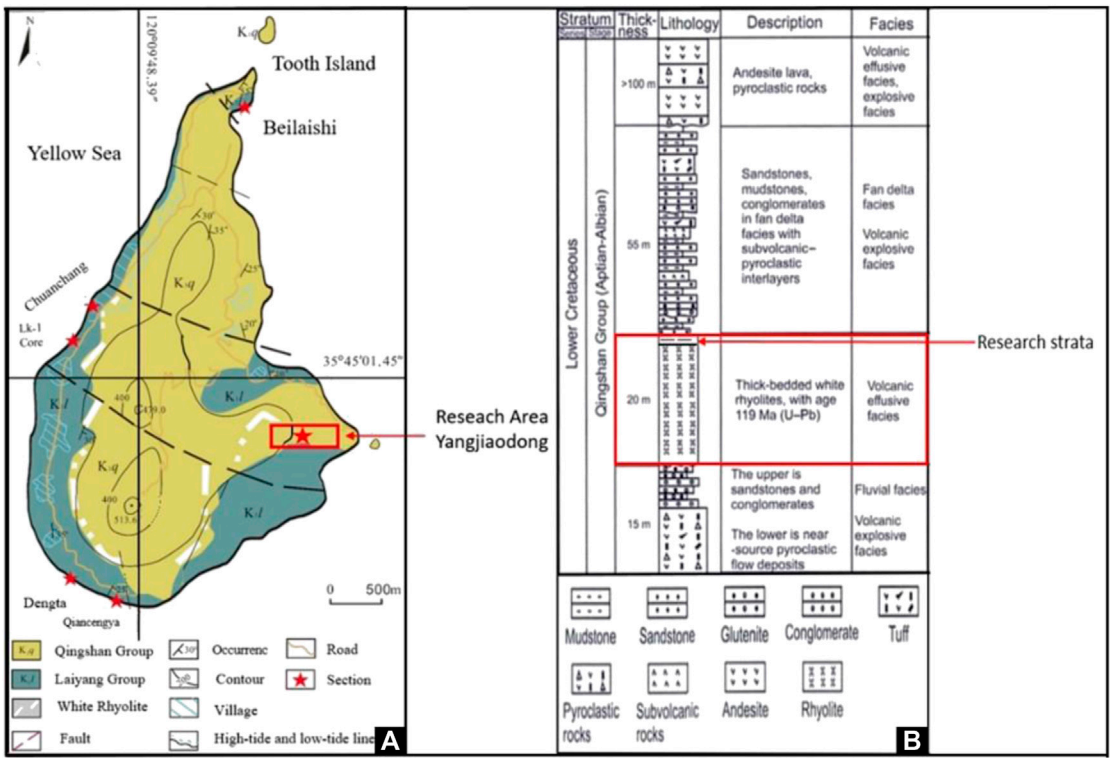

FIGURE 2 | Geological survey of Lingshan Island (Revised after Luan, 2010) and profile of the Qingshan Group strata in the Yangjiaodong section of Lingshan Island, Shandong Province (Revised after Peng, 2017).

and U and depletion of Nb, Ta, Hf, and P, reflecting the mature evolution of magmatic rocks in the Qingshan period (Dong et al., 2019). The distribution of light and heavy rare earths is weak. Eu and Sr are considerably negative anomalies. Light rare earth elements are relatively enriched, and heavy rare earth elements are relatively slightly depleted, suggesting that feldspar may have been fractionally crystallized during diagenesis (Zhang et al., 2019). These geochemical characteristics indicate that the rhyolite was formed in an environment of extensional decompression (Ao et al., 2018).

Research on the formation age of Lingshan Island strata produced precise chronology evidence. By using the zircon U–Pb dating method, Zhou et al. (2015) determined that the absolute age of rhyolite on the island is approximately 119.2 ± 2.2 Ma, indicating the late Early Cretaceous Qingshan stage magmatic activity. The source identified by Hf isotope indicates the partial melting of the ancient crust (Ao et al., 2018).

3 SAMPLING AND SIMULATION ANALYTICAL METHOD

The onsite investigation of Lingshan Island, Yangjiaodong (N35°45′16.38″, E120°11′12.00″) demonstrated that the gray–white rhyolite and the upper rhyolitic tuff have apparent rhythm. The samples were collected from a 46.6-cm-long tuff outcrop above the white rhyolite. A thin section was prepared from fresh-cut surface of the sample and microscopically examined. A scale was used to measure the thicknesses of different lithologies and classify statistics using Acycle2.3 software to perform time series analysis and filtering mapping. Acycle is software designed for astronomical cycle analysis, with powerful data processing functions. It can interpolate, detrend, and spectrum analyze of discrete nonlinear data similar to the data obtained in this study (Huang, 2014; Li, et al., 2019; Yang et al., 2021). The field measurement data obtained in this study are dispersed and numerous (Data appendix), even if it is limited to identification and analysis of a certain time span of volcanic eruptions, rather than the large-scale magmatic dynamics process.

The analysis model sets the thickness of the tuffaceous rhyolite layer of the sample to represent the eruption scale, and the thickness of the mud layer represents the dormant time of volcanism. For the deep-time volcanism, the current chronology cannot accurately depict the millennium scales. Therefore, the analysis method of volcanic cycle stratigraphy is undertaken to establish a high-precision magmatic activity time frame related to volcanism and the time-scale sequence analysis of the collected samples is conducted using Acycle software. Signal analysis software performs interpolation, detrending, spectrum analysis, and filtering of quantitative data, obtaining continuous signal curve, which proves that the magma chamber is always in an active

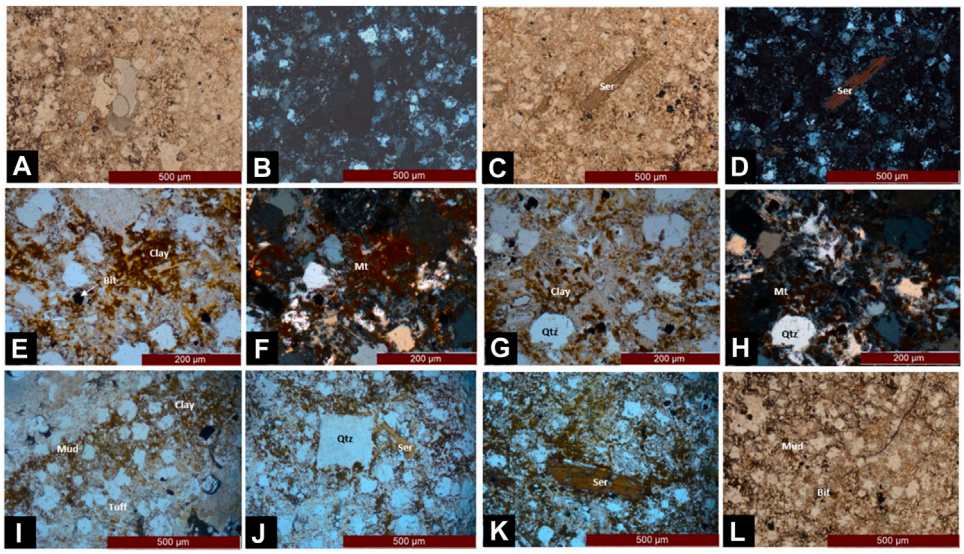

FIGURE 3 | Petrographic characteristics of the mud rock sample in Lingshan Island. [**(A)** Single polarizer about silicified. **(B)** Orthogonal polarizer about silicified. **(C)** Sericite single polarizer. **(D)** Sericite orthogonal polarizer. **(E)** Single polarizer. **(F)** Iron minerals orthogonal polarizer. **(G)** Clay single polarizer. **(H)** Orthogonal polarizer. **(I)** Interbedded single polarizer. **(J)** Self-shaped quartz single polarizer. **(K)** Single polarizer. **(L)** Silicified quartz orthogonal polarizer].

state over a scale of millennium years. Then, the power spectrum method is used to separate the wave information of continuous signal periods and obtain the activity status of different scales and periods within the magma chamber.

4 ANALYSIS AND RESULTS

4.1 Petrographic Analysis

Small pieces were collected from samples for thin section grinding, and thin sections were prepared by longitudinal and transverse cutting, depending on the rock sample characteristics. Microscopic observation showed interbedded light tuff and dark mudstone, quartz, red iron minerals, and brown clay minerals (**Figure 3I**). Deep brown tuff belt with stripes can be observed in a longitudinal section (**Figure 3I**); whereas cross sectional cut thin section show dark tuff layers, mica, quartz, calcite, and clay minerals embedded around the quartz (**Figure 3C,E,G,J,K**). Some thin sections have visible pyroclastic structures with varying sizes of quartz, potassium feldspar phenocrysts, and plastic debris (**Figure 3A,H**). Debris and breccia comprises andesite (**Figure 3K**, l); crystal debris is subrhombohedral plagioclase with volcanic ash cementation (**Figure 3E,F**). The thin sections contain sericite, plagioclase, potassium feldspar, spinel, and esite, and other minerals (**Figure 3F,G,K**). The black particles observed under the microscope are sodium ferroamphibole, biotite, and possibly a small amount of magnetite, indicating magma contamination (**Figure 3H,J,K**). The binding material is mainly dacite and sandstone cuttings. The sample lithology is classified as rhyolitic tuff and mudstone.

4.2 Statistical Analysis of Lithology of Rock Samples

4.2.1 Preliminary Data Processing

The layers of rhythmic samples collected in the Yangjiaodong area of Lingshan Island were measured and counted. The lithology of the samples was divided into mud and tuff, and the thicknesses of each layer at the top and bottom layers were noted and recorded (Data appendix). The tuff layer thickness represents the size of the volcano eruption. The conversion of mudstone thickness represents the dormant time of the volcanic eruption. Because the original sample do not show the thickness and relative position of each lithology clearly (**Figure 4**), the sample was digitally processed and the relative thickness of the two lithologies were obtained, as shown in **Figure 5A**, which represents alternation volcanic eruptions and volcanic intermittent periods. Then, the two lithology histograms were superimposed to assess the trend of volcanism from a macro perspective. As shown in **Figure 5B**, the geological process recorded by this sample is dominated by the volcanic eruption, and there are several long dormant periods.

Sample thicknesses were measured after compaction. According to the petrographic observation results, the dark layer of the sample is mudstone. After the long geological process, the present exposed thickness is not the original thickness of volcanic ash erupted at that time, so the research results on mudstone compaction factor are searched and the average value is calculated. So the average compaction factor of mudstone is 0.3 (Yang et al., 2019), which indicates that the sedimentary thickness of the sample at the time of formation is approximately three times the present outcrop. Second, the interval time span has a geological meaning. Combined with the geological setting of the region, Late Mesozoic offshore rift basin, the

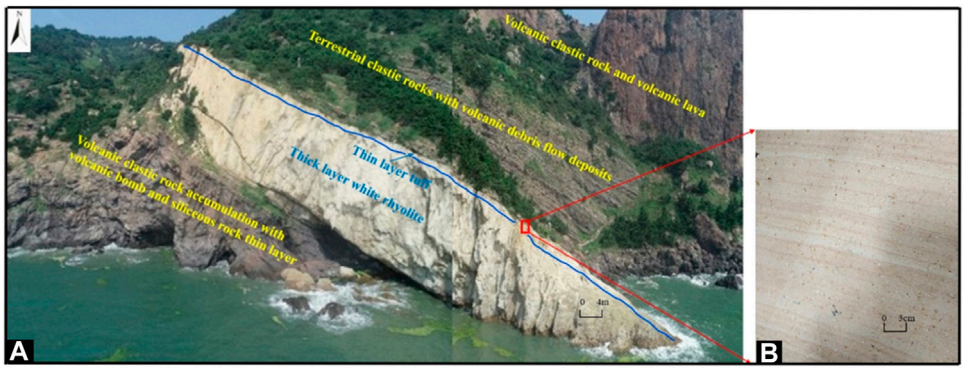

FIGURE 4 | (A): Field photos of Yangjiaodong profile on Lingshan Island; **(B)**: Partial photo of rock slate sample.

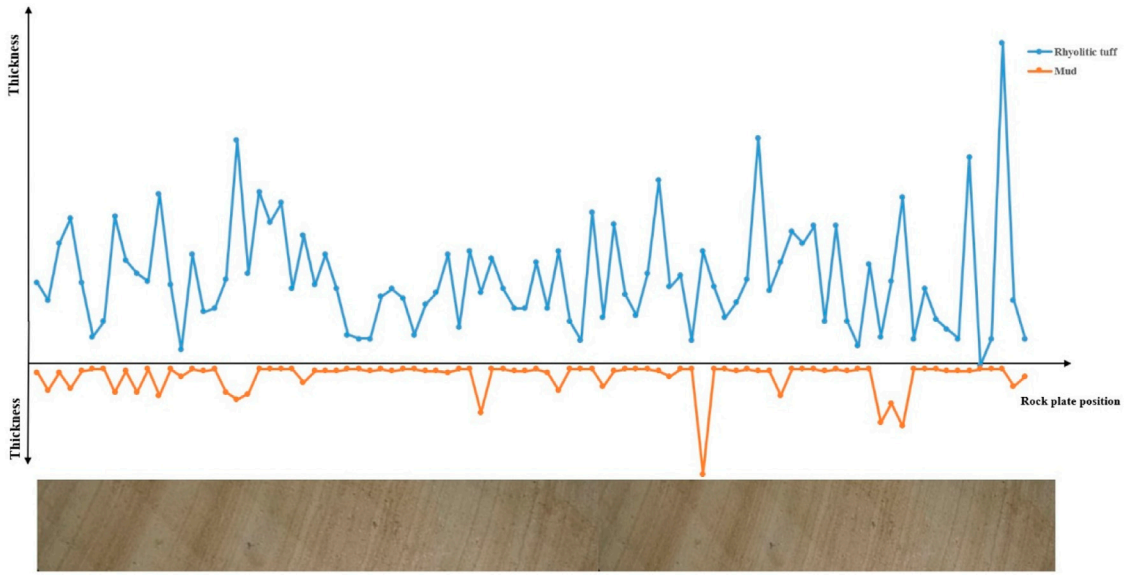

FIGURE 5 | Lithologic line chart of the Lingshan Island sample and whole-rock plate.

sedimentary rate of the volcanic back-arc basin with insufficient source supply (Ma et al., 2018) was found and an average value of 6.5 m/Ma was considered. This rate is also an approximate reference value selected according to the characteristics of Mesozoic rift basins in Ri-Qing-Wei Basin. After determining the aforementioned two factors, the original measurement data were processed to determine the time span of volcanic activity within the sample range to be approximately 2.24 Ma, and the cumulative eruption thickness of volcanic ash was approximately 1.4 m.

First, the time data sequence analysis, the cumulative time, and a single mudstone sedimentary layer as abscissa and ordinate were fed into Acycle software. Second, the scale data were processed in the same method.

4.2.2 Acycle Spectrum Analysis and Filtering Mapping

Because there are 180 original measurement data, lithology classification statistics can be divided into two groups, first the 90 data points of argillaceous sedimentary rocks using Acycle software version 2.3 data interpolation, detrending, and spectrum analysis of several steps to obtain the power spectrum per millennium (Li, et al., 2019). Acycle is a data analysis software jointly developed by Professor Mingsong Li of Peking University and American cyclic stratologist Linda A. Hinnovv in 2019. It has solved many scientific problems, mainly involving the marine deposition of the Milakovich cycle (Liu et al., 2021), and the graphical calculation of the deposition rate of the terrigenous clastic cycle (Yang et al., 2021). This software can analyze discrete data, which can be combined into continuous-time signals. The periodic information in fast Fourier transform diagrams and power spectrum diagrams are identified to solve the problems presented by the discreteness of geological data vs. the typical data that can be identified by the computer.

As shown in **Figure 6A**, the transverse coordinate values (frequency size) of the four points with the highest energy

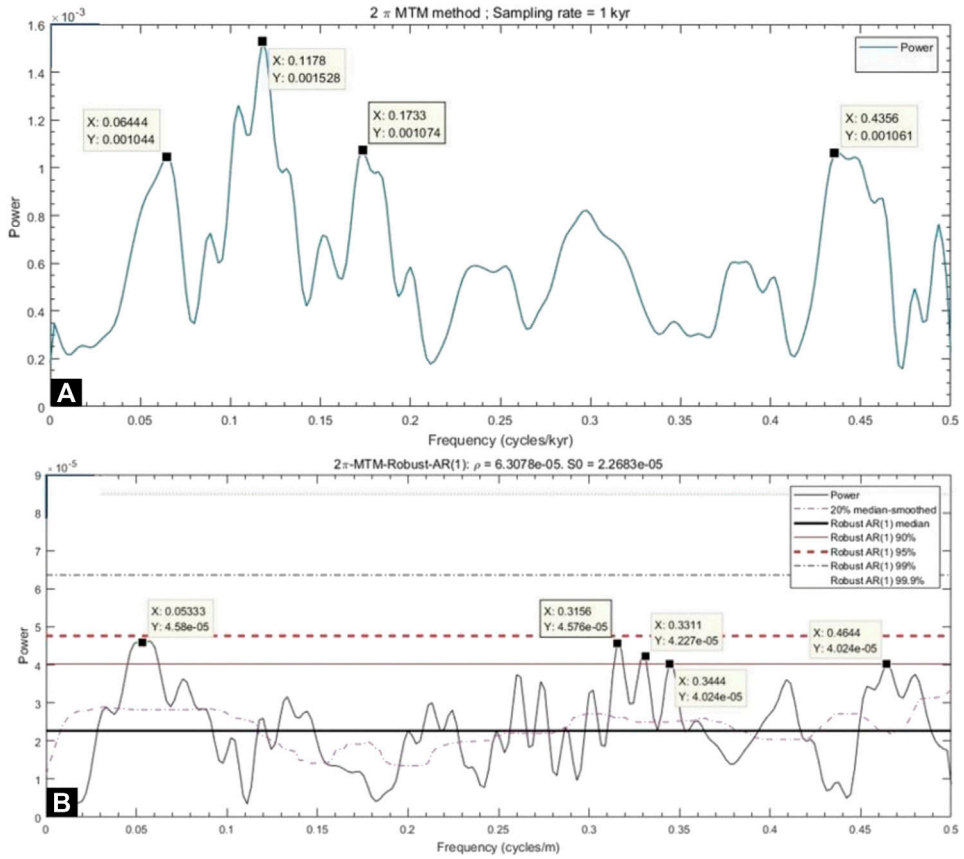

FIGURE 6 | Time series analysis power spectrum and scale analysis power spectrum.

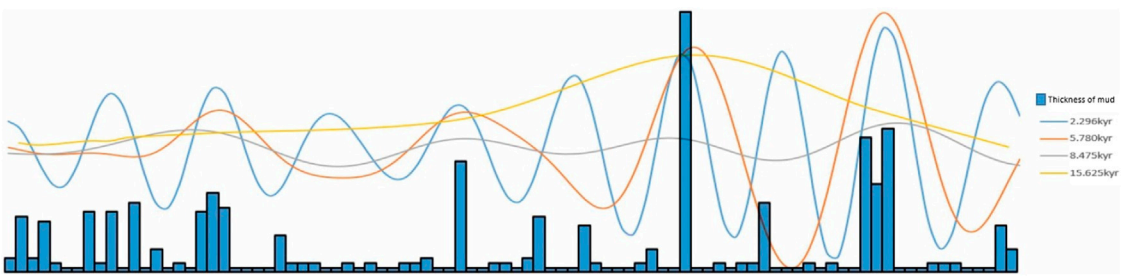

FIGURE 7 | Column chart of mudstone thickness and the time series analysis curve.

(power is large) on the power map are calculated. The known *Period =1/Frequency*, and the four periods are 2.296, 5.78, 8.475, and 15.625 kyr. The calculation results show that the probability of these four cycles is the highest in the time range shown in the rock sample. As for the calculation of scale, the two points (0.3156 and 0.3311) which are closer to the numerical value are combined to obtain an average of four scales: 2.17, 2.94, 3.12, and 18.87 m, which indicate that these four eruption scales exist within the thicknesses represented by the rock samples.

According to the cycle data, the original curve is filtered and matched with the original digital mudstone thickness map to obtain **Figure 6**, verifying the accuracy of cycle identification. **Figure 7** shows that the minimum cycle (2.296 kyr) has gone through nine cycles, which is consistent with the total time span of the collected samples of 2.24 Ma. The corresponding 5.78 kyr has roughly four cycles, 8.475 kyr has approximately three cycles, and 15.625 kyr has only one cycle. It shows that the longest cycle (15.625 kyr) has not experienced a complete cycle in the volcanic eruption event represented by the sample. If the activity is maintained under ideal conditions, the longest cycle can be completed.

The results of scale analysis represent the thickness of volcanic ash deposition during each volcanic eruption; however, the thickness

TABLE 1 | Comparison result of magma chamber parameters.

Pressure/MPA	Melt/%Vol	Crystallinity/1	Eruption scale/M	Temperature/°c	Water/wt%
200	50	0.6	18.87	800	3.5
160	40	0.5	3.12	770	3
155	35	0.45	2.94	760	2.5
150	30	0.4	2.17	750	2

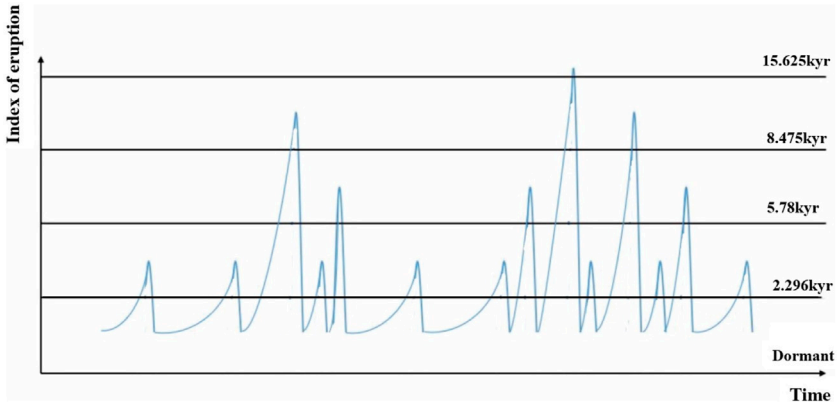

FIGURE 8 | Pulse pattern map of the volcanic eruption in the Yangjiaodong area of Lingshan Island.

is considerably reduced because of the external compaction over a thousand years. The thickness of the sample is not fully consistent. The calculation shows that the minimum scale (2.17 m) experienced roughly two cycles, and the corresponding 2.94 and 3.12 m experienced about one cycle; the largest scale (18.87 m) experienced 0.2 cycles. The four results obtained from the scale analysis were used to determine the volcanic eruption process (Feng et al., 2021) by combining the conditions that limit the magma chamber eruption conditions with the rheological lockup window, the reduction of activity due to the low melt in the magma is limited by the crystal formation (Feng et al., 2021).

5 DISCUSSION

5.1 Possible Cause of Volcanic-Sedimentary Rhythm-Dynamic Evolution of Melt

There are different volcanic eruptions in a certain period accompanied by underground deep magmatic movement processes. The magma can continuously enter the near-surface magma storage only during the active state. The melt is the symbol to identify the magma activation. The dynamic evolution process of the melt can be summarized as follows: first, the production of the melt: in the vacuum degassing environment of the magma chamber, it may be the transformation of the precrystal to form the melt; it is also possible that partial crystallization forms water-containing melt (Annen et al., 2006). Second, the remobilization mechanism of melt: only the activated melt can move upward, which may be the periodic supplement of heat source and long-term thermal contact (Cooper and Kent, 2014); it is possible that the gas permeability and magmatic contact interfaces with different properties are the upward heat absorption of near-solid magma (Bachmann and Bergantz, 2004). Finally, the self-changing mechanism of the melt: the activated melt needs to reach the corresponding temperature further, and pressure conditions to move upward and finally form highly differentiated magma. The rate of magmatic differentiation can be quantified based on the crystallization characteristics of minerals at different stages (Rubin et al., 2017; Karakas et al., 2019); the relative amount between the melt content and rheological lockup state can also be calculated for determining the change in magma chamber temperature (Jackson et al., 2018.; Zhao, 2021; Zhao.et al., 2021).

Combined with the study of these three parts, the theory can be transferred to the deep dynamic evolution process of melt, the process of forming highly differentiated magma to simulate the deep dynamic evolution process of the melt. The melt indicates magma activation and undergoes three stages: generation, mobilization, and self-change. Finally, the magma surges to the near-surface magma chamber for temporary storage, and the temperature and pressure conditions meet the time of the intermittent eruption (Schaen et al., 2021). The amount of each eruption in the magma chamber only occupies a small part of the total volume of the magma chamber. The continuous activation of the melt floats up and down the rheological locking window. In this process, the magma continuously differentiates, changes in composition, and finally ejects from the surface in the form of highly differentiated magma (Wotzlaw et al., 2022). The pulsed volcanic eruption state underwent during this period indicates

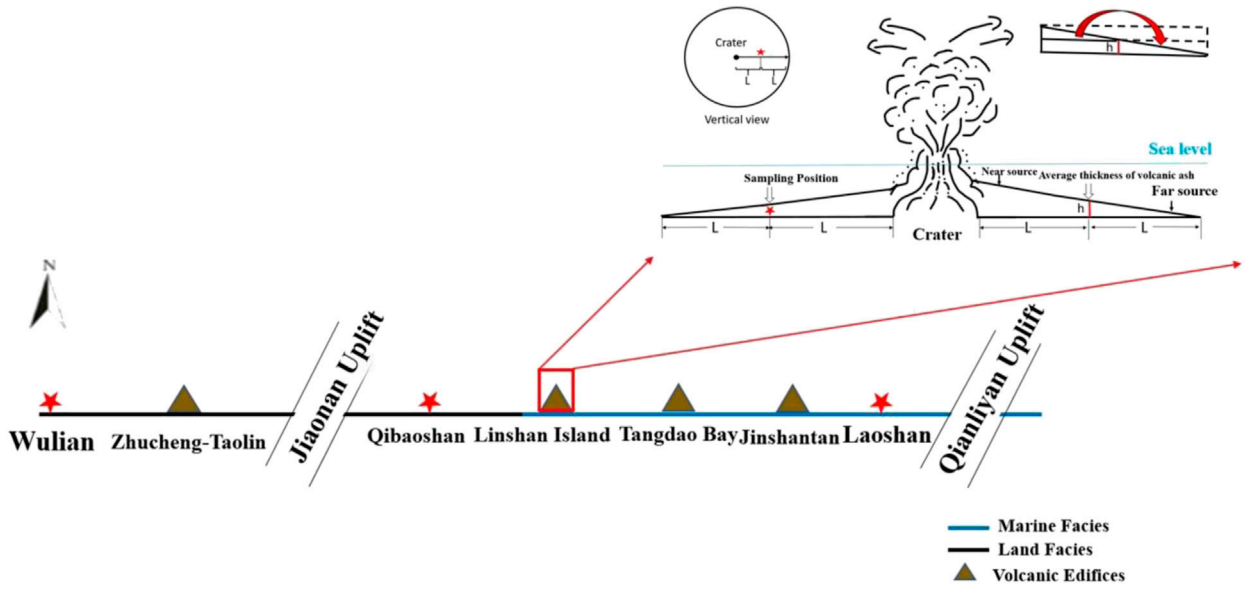

FIGURE 9 | Volcanic edifice diagram of Lingshan Island and the offshore area in eastern Shandong Province.

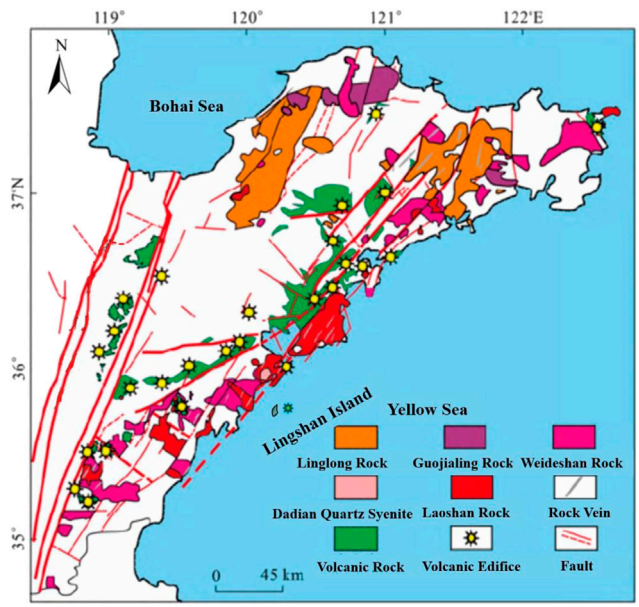

FIGURE 10 | Map of volcanic edifices in the offshore of eastern Shandong Province (Revised after Zhou et al., 2018).

underground magma chamber activity reflected on the surface. The volcanic eruption process is quantified *via* numerical analysis, proving the availability of the applying to power spectrum analysis in volcanology.

The magma erupts depending on whether the melt in the magma chamber reaches the rheological lockup window (magma crystallinity >0.6). The premise for forming highly differentiated granite is that the temperature and pressure conditions repeatedly fluctuate up and down the rheological locking window. The general conditions for eruption were found through previous studies: temperature 750–800°C; water content 2–3.5wt%; pressure 150–200MPa; melt content 30–50%vol; and magma crystallinity 0.4–0.6. The farther the magma chamber is from the surface, the higher the temperature and pressure conditions are required. Based on this theory, the rheological locking points of four eruption modes are determined (Zhao, 2021; Zhao et al., 2021; Zhao et al., 2021). In this study, because the rock samples show good rhythm, indicating that the composition of the magma did not change sufficiently; therefore, the rhythm layer is the product of the physical process of magmatic eruption dynamics and is an indication of volcanic eruption dynamics.

With the progress of time, the temperature and pressure conditions in the magma chamber will continue to change. The previous magma eruption might affect the next volcanic activity, and the previous eruption can block the magma channel or create conditions for the next eruption, that is, the continuous curve is the magmatic activity signal, and the peak is the superposition of several different periods of signals. This study identifies the time signal and explains it with reasonable geological facts. Combined with the previous calculation cycle results (four periods: 2.296, 5.78, 8.475, and 15.625 kyr), the conditions of volcanic eruption in the study area are roughly defined: Condition one (temperature: 750°C, water content: 2 wt%, pressure: 150 MPa, melt content: 30% vol, and magma crystallinity: 0.4); Condition two (temperature: 760°C, water content: 2.5 wt%, pressure: 155 MPa, melt content: 35% vol, and magma crystallinity: 0.45); Condition three (temperature: 770 °C, water content: 3 wt%, pressure: 160 MPa, melt content: 40% vol, and magma crystallinity: 0.5); and Condition four (temperature: 800 °C, water content: 3.5 wt%, pressure: 200 MPa, melt content: 50% vol,

and magma crystallinity: 0.6). The division (**Table 1**) of these four eruption conditions is only an assumption aimed at completing the impulsive eruption model (**Figure 8**), which is a preliminary study about the limiting conditions of magmatic dynamics. **Figure 8** shows that the form of volcanic eruption in the study area shows the characteristics of pulse change, reflecting the periodicity and cyclicity of volcanic eruptions.

Therefore, the generation of rhyolitic tuff in Lingshan Island is a series of upwelling and underplating of magma carrying melt, resulting in numerous new magma chamber produced by the partial melting process of overlying ancient crustal material in the shallow extension environment. Then this part of magma and asthenosphere mantle material rise to the surface along the fault zone, and a high degree of differentiation and evolution occurs in the process of rising (Zhang et al., 2019). After the temperature and pressure conditions are satisfied, magma erupts according to specific rules. During this period, sedimentation occurs continuously, making the surface show rhythmic lithologic interbedding. In summary, it is attempted to draw the volcanic rhythm pattern of white rhyolitic tuff in the Yangjiaodong area of Lingshan Island.

Being affected by many uncertain factors, such as tectonism and external heat source heating, the conditions such as temperature and pressure in the magma chamber are constantly changing; therefore, the eruption situation presents diversity.

5.2 Characteristics of Volcanic Edifices Around Lingshan Island

Based on the rhythmic characteristics of rhyolitic tuff in Yangjiaodong of Lingshan Island, and the volcanic edifices research in Wulian (E119°12′), Zhucheng-Taolin (E119°30′12″), Qibao Mountain (E119°55′), Lingshan Island (E120°11′12″), Tangdao Bay (E120°11′42″), Jinshatan (E120°14′15″), and Laoshan (E120°38′38″) areas in the area of eastern Shandong Province (**Figure 9**), under the guidance of the theory of trans-crustal magmatic system, in the eastern of Shandong Province, the late Mesozoic volcanic activity is strong and the cyclicity is obvious. The volcanic edifices are beaded along the Qingdao–Wulian fault and Muping–Jimo fault. Zhou et al., 2015; 2018), indicated that the volcanic activity of the Early Cretaceous Qingshan period began with the eruption of acidic volcanic rocks, namely, the white rhyolitic tuff in Lingshan Island (Liang et al., 2015; Zhang et al., 2015; Zhang, 2017). Each eruption of volcano releases numerous volcanic materials. The thickness of volcanic ash decreases from near to more distant areas after falling. In addition, an approximately circular region with a radius of approximately twice the distance (2 L) is formed near the sampling point. This is because the erupted material is volcanic overflow tuff facies and coexists with rhyolite; therefore, the distance from the crater will not be too far from the sampling point. As shown in **Figure 10**, from the overall point of view of the eastern coastal areas of Shandong Province, the volcanic institutions are projected into the same east–west line, forming a schematic diagram of the volcanic institutions in the eastern coastal areas of Shandong Province, which is extended from the sampling location characteristics of Lingshan Island to other regions. As shown in **Figure 9**, Lingshan Island is located in the middle of the above volcanic edifices. The correlation between the identified four cycles and these craters is that in the early Cretaceous Qingshan period (120 Ma), these areas are the outcrop positions at the end of the trans-crustal magmatic system, the volcanic mechanism formed by volcanic ash that magma up to the surface through the cracks. Therefore, the identified four cycles may represent the eruption characteristics of volcanoes in Qibao Mountain, Taolin, Lingshan Island, and Tangdao Bay in the Early Cretaceous.

6 CONCLUSION

The rhyolitic tuff mudstone interbedded profile developed in the Yangjiaodong area of Lingshan Island reflects the rhythm of the Early Cretaceous magmatic eruption.

Software Acycle numerical analysis method power spectrum enables prediction of the characteristics of the research area volcanic edifices. The following conclusions are drawn: the magma stored in the magma chamber in the Yangjiaodong area of Lingshan Island erupted according to certain conditions (melt parameters: temperature, water content, pressure, melt content, and magma crystallinity). In 2.24 Ma time frame, the volcanic eruption cycle occurred in four periods of different lengths (2.296, 5.78, 8.475, and 15.625 kyr) appearing alternately. In general, the early stage is dominated by small scale, and the late stage is characterized by volcanic events of alternating size, showing the pulse volcanic eruption formation. The scale of volcanic eruption also has the characteristics of size (2.17, 2.94, 3.12, and 18.87 m). Based on the two kinds of results, we speculate the characteristics of volcanic eruption in the coastal area of eastern Shandong province: volcanic overflow sedimentary system with pulse eruption as the dynamic characteristics.

DATA AVAILABILITY STATEMENT

The original contributions presented in the study are included in the article/**Supplementary Material**; further inquiries can be directed to the corresponding authors.

AUTHOR CONTRIBUTIONS

All authors listed have made a substantial, direct, and intellectual contribution to the work and approved it for publication.

FUNDING

This work was supported by the Project of Department of Science and Technology of Sinopec (No. P20028), the Teacher Innovation Project (grant no. 19CX05004A), Shaanxi Youth Science and Technology Star Project (Grant No. 2021KJXX-87), Shaanxi

public welfare geological survey project (Grant No. 20180301), and SINOPEC Petroleum Exploration and Production Research Institute open fund (HX20220005).

ACKNOWLEDGMENTS

The authors would like to thank Beijing GeoAnalysis Co., Ltd. for their invaluable technical support. We are grateful to the reviewers for their constructive, careful, and stimulating reviews.

SUPPLEMENTARY MATERIAL

The Supplementary Material for this article can be found online at: https://www.frontiersin.org/articles/10.3389/feart.2022.908193/full#supplementary-material

REFERENCES

Annen, C., Blundy, J. D., and Sparks, R. S. J. (2006). The Genesis of Intermediate and Silicic Magmas in Deep Crustal Hot Zones. *J. Petrology* 47 (3), 505–539. doi:10.1093/petrology/egi084

Ao, W. H., Feng, T., Zhao, Y., Zhai, M. G., and Sun, Y. (2018). Early Cretaceous Magmatic Activities in the Lingshan Island and its Geological Significance. *Acta Petrologica Sinica* 34 (6), 1612–1640 (in Chinese with English abstract).

Bachmann, O., and Bergantz, G. W. (2006). Gas Percolation in Upper-Crustal Silicic Crystal Mushes as a Mechanism for Upward Heat Advection and Rejuvenation of Near-Solidus Magma Bodies. *J. Volcanol. Geotherm. Res.* 149 (1-2), 85–102. doi:10.1016/j.jvolgeores.2005.06.002

Cashman, K. V., Sparks, R. S. J., and Blundy, J. D. (2017). Vertically Extensive and Unstable Magmatic Systems: a Unified View of Igneous Processes. *Science* 355 (6331), eaag3055. doi:10.1126/science.aag3055

Cooper, K. M., and Kent, A. J. R. (2014). Rapid Remobilization of Magmatic Crystals Kept in Cold Storage. *Nature* 506 (7489), 480–483. doi:10.1038/nature12991

Dong, S. (2020). *Characteristics of Melting Inclusions of Cretaceous Qingshan Group Volcanic Rocks in the Coastal Area of Eastern Shandong*. East China: China University of Petroleum.

Dong, S., Zhou, Y., Liang, Z., Zhou, T., An, Y., and Gu, Y. (2019). Geochemical Characteristics and Geological Significance of Siliceous Rocks in Qingshan Group, Lingshan Island, Shandong. *Geochem. Rep. Mineral Rocks* 38 (3), 623–633. doi:10.19658/j.issn.1007-2802.2019.38.051

Doucet, L. S., Li, Z.-X., Ernst, R. E., Kirscher, U., El Dien, H. G., and Mitchell, R. N. (2020). Coupled Supercontinent-Mantle Plume Events Evidenced by Oceanic Plume Record. *Geology* 48 (2), 159–163. doi:10.1130/G46754.1

Feng, Z., Sun, D.-Y., and Gou, J. (2021). Differentiation of Magma Composition: Reactivation of Mush and Melt Reaction in a Magma Chamber. *Lithos* 388-389, 106066. doi:10.1016/j.lithos.2021.106066

Feng, Z., Sun, D. Y., Yue, Y., Mao, A. Q., Tian, L., Sun, C., et al. (2020). Petrogenesis of Highly Differentiated I-type Volcanic Rocks: Reinjection of High-temperature Magma-An Example from Suolun Silicic Volcanic Rocks, Central Great Xing'an Range, China. *Geol. J.* 55 (10), 6677–6695. doi:10.1002/gj.3838

Hofmann, A. W. (2012). Magma Chambers on a Slow Burner. *Nature* 491 (7426), 677–678. doi:10.1038/491677a

Huang, C. (2014). Stratigraphy and Chronology and Their Research Status in Mesozoic. *Geosci. Front.* 21 (02), 48–66. doi:10.13745/j.esf.2014.02.005

Jackson, M. D., Blundy, J., and Sparks, R. S. J. (2018). Chemical Differentiation, Cold Storage and Remobilization of Magma in the Earth's Crust. *Nature* 564 (7736), 405–409. doi:10.1038/s41586-018-0746-2

Karakas, O., Wotzlaw, J.-F., Guillong, M., Ulmer, P., Brack, P., Economos, R., et al. (2019). The Pace of Crustal-Scale Magma Accretion and Differentiation beneath Silicic Caldera Volcanoes. *Geology* 47 (8), 719–723. doi:10.1130/g46020.1

Li, M., Hinnov, L., and Kump, L. (2019). Acycle: Time-Series Analysis Software for Paleoclimate Research and Education. *Comput. Geosciences* 127, 12–22. doi:10.1016/j.cageo.2019.02.011

Liang, W. (2016). *Evolution Characteristics of the Late Mesozoic Volcanic-Magma System in the Offshore Area of Eastern Shandong*. East China): China University of Petroleum.

Liang, W., Zhou, Y., Zhang, Z., and Zhou, T. (2015). Early Cretaceous Magmatic Evolution Characteristics of Coastal Rift Basins in Eastern Shandong. *Abstr. Pap. 15th Annu. Conf. China Soc. Mineral Rock Geochem.* 1, 167–168.

Liu, D., Huang, C., Kemp, D. B., Li, M., Ogg, J. G., Yu, M., et al. (2021). Paleoclimate and Sea Level Response to Orbital Forcing in the Middle Triassic of the Eastern Tethys. *Glob. Planet. Change* 199, 103454. doi:10.1016/j.gloplacha.2021.103454

Liu, F., Zhou, Y., Xu, H., and Zhang, Z. (2016). The Genetic Characteristics, Types and Geological Tectonic Significance of Lingshan Island. *Mar. Geol. front* 32 (03), 33–40. doi:10.16028/j.1009-2722.2016.03005

Liu, J., Ni, J., Chen, X., Jp, C., Zheng, Y., Sun, Y., et al. (2020). Parallel Extension Tectonics: Mechanism of Early Cretaceous Thinning and Destruction of the Lithosphere of the North China Craton. *Acta Petrol. Sin.* 36 (8), 2331–2343. doi:10.18654/1000-0569/2020.08.04

Luan, G., Li, A., Wang, J., Gan, L., and Xie, R. (2010). Genetic Classification and Geological Environment Analysis of Major Islands in Qingdao. *J. Ocean Univ. China (Natural Sci. Ed.* 40 (08), 111–116. doi:10.16441/j.cnki.hdxb.2010.08.018

Ma, C., and Li, Y. (2017). Cumulative Growth of Granites and Differentiation of High Crystallinity Magma. *Acta Petrol. Sin.* 33 (05), 1479–1488. doi:10.1007/s10114-017-6556-x

Ma, C., Zou, B., and Gao, K. (2020). Storage of Porridge, Cumulative Assembly of Intrusive Bodies and Genesis of Granite. *Earth Sci.* 45 (12), 4332–4351. doi:10.3799/dqkx.2020.316

Ma, X., Deng, S., Fan, R., and Lu, Y. (2018). Research on Cyclic Stratigraphy of the Baota Formation of the Upper Ordovician in Xishui, Guizhou. *Palaeontol. Soc. China*, 1. Summarized papers of the Twelfth National Congress of the Chinese Palaeontological Society and the 29 th Annual Academic Conference. Palaeontological Society of China : Palaeontological Society of China.

Meng, Y., and Li, R. (2019). Early Cretaceous Tectonic Evolution of Lingshan Island and its Adjacent Areas in Qingdao. *Geol. Rev.* 65 (02), 385–388. doi:10.16509/j.georeview.2019.02.021

Meng, Y., Li, R., Yang, X., and Hou, F. (2018). Zircon U-Pb-Hf Isotopic Characteristics and Tectonic Significance of Early Cretaceous Clastic Rocks in Lingshan Island, Qingdao, Shandong. *Geoscience* 43 (09), 3302–3323. doi:10.3799/dqkx.2018.207

Reubi, O., and Blundy, J. (2009). A Dearth of Intermediate Melts at Subduction Zone Volcanoes and the Petrogenesis of Arc Andesites. *Nature* 461 (7268), 1269–1273. doi:10.1038/nature08510

Rubin, A. E., Cooper, K. M., Till, C. B., Kent, A. J., Costa, F., Bose, M., et al. (2017). Rapid Cooling and Cold Storage in a Silicic Magma Reservoir Recorded in Individual Crystals. *Science* 356 (6343), 1154–1156. doi:10.1126/science.aam8720

Schaen, A. J., Schoene, B., Dufek, J., Singer, B. S., Eddy, M. P., Jicha, B. R., et al. (2021). Transient Rhyolite Melt Extraction to Produce a Shallow Granitic Pluton. *Sci. Adv.* 7 (21), eabf0604. doi:10.1126/sciadv.abf0604

Sun, M., Chen, H., Milan, L. A., Wilde, S. A., Jourdan, F., and Xu, Y. (2018). Continental Arc and Back-arc Migration in Eastern NE China: New Constraints on Cretaceous Paleo-Pacific Subduction and Rollback. *Tectonics* 37 (10), 3893–3915. doi:10.1029/2018tc005170

Wang, L., Ren, T., Liu, H., Ning, Z., Yu, X., Guo, R., et al. (2021). Mesozoic Granite Division in Jiaodong Area. *Shandong land Resour.* 37 (08), 1–14.

Wang, S., Wang, X., and Du, D. (2020). Volcanic Rock-Intrusive Rock Contact. *Univ. Geol. J.* 26 (5), 497–505. doi:10.16108/j.issn1006-7493.2020014

Wotzlaw, J. F., Bastian, L., Guillong, M., Forni, F., Laurent, O., Neukampf, J., et al. (2022). Garnet Petrochronology Reveals the Lifetime and Dynamics of

Phonolitic Magma Chambers at Somma-Vesuvius. *Sci. Adv.* 8 (2), eabk2184. doi:10.1126/sciadv.abk2184

Wu, F., Liu, X., Ji, W., Wang, J., and Yang, L. (2017). Identification and Research of Highly Differentiated Granites. *Chin. Sci. Earth Sci.* 47, 745–765. doi:10.1360/N072016-00139

Yang, C., He, Y., and Lei, Y. (2019). Compaction Coefficient and Paleopressure Characteristics of Triassic Yanchang Formation Mudstone in Southern Ordos Basin. *J. Xi 'an Univ. Sci. Technol.* 39 (6), 992–998. doi:10.13800/j.cnki.xakjdxxb.2019.0611

Yang, Y., Fu, W., Yu, J., Ning, Z., Cui, J., Li, Q., et al. (2021). Cyclostratigraphical Analysis of Continental Red Beds Below K/Pg Boundary in the Jiaolai Basin. *Acta Sedimentologica Sinica* 39 (4), 942–952. doi:10.14027/j.issn.1000-0550.2020.046

Zhang, H., Lu, H., Li, J., Wang, J., Zhang, S., Dong, X., et al. (2013). Shandong Qingdao Early Cretaceous New Stratigraphic Unit-Lingshandao Formation. *Stratigr. J.* 37 (02), 216–222. doi:10.19839/j.cnki.dcxzz.2013.02.012

Zhang, S., Meng, Y., and Wang, Z. (2019). A New Understanding of the Petrogenesis and Tectonic Environment of Rhyolites in Lingshan Island, Qingdao, Shandong. *Coll. Geol. J.* 25 (05), 654–669. doi:10.16108/j.issn1006-7493.2019019

Zhang, Z. (2017). *Tectonic-magmatic Evolution Sequence and Lithosphere Dynamics of Riqingwei Basin*. East China): University of Petroleum of China.

Zhang, Z., Zhou, Y., and Liang, W. (2015). Late Mesozoic Magmatic Evolution History in Eastern Shandong. *Geol. Rev.* 61 (S1), 778–779.

Zhang, Z. M., Ding, H. X., Dong, X., and Tian, Z. L. (2020). Partial Melting of Subduction Zones. *Acta Petrol. Sin.* 36 (9), 2589–2615. doi:10.18654/1000-0569/2020.09.01

Zhao, F. (2021). *Early Cretaceous Felsic Magma Chamber Process in Central Daxinganling: A Case Study of Igneous Rocks in Baiyintao Basin*. Changchun,China: Jilin University.

Zhao, L., Guo, F., Zhang, X., and Wang, G. (2021). Cretaceous Crustal Melting Records of Tectonic Transition from Subduction to Slab Rollback of the Paleo-Pacific Plate in SE China. *Lithos* 384, 105985. doi:10.1016/j.lithos.2021.105985

Zhou, Y., Zhang, Z., Liang, W., Su, L., and Yue, H. (2015). Late Mesozoic Tectonic-Magmatic Activity and Prototype Basin Restoration in Eastern Shandong. *Geol. Front.* 22 (01), 137–156. doi:10.13745/j.esf.2015.01.012

Zhou, T. F., Zhou, Y. Q., Søager, N., Holm, P. M., and Zhang, Z. K. (Forthcoming 2022). Late Mesozoic Rifting and its Deep Dynamic Mechanisms in the Central Sulu Orogenic Belt: Records from Lingshan Island. *Sci. China Earth Sci.* doi:10.1360/SSTe-2021-0061

Zhou, Y., Zhou, T., Ma, C., Zhang, Z., Dong, S., Gu, Y., et al. (2018). Transcrustal Magmatic System of Early Cretaceous (Qingshan Stage) in Eastern Shandong and the Basin Formation Related to 'Thermal Upwelling-Detachment'. *Earth Sci.* 43 (10), 3373–3390. doi:10.3799/dqkx.2018.998

Zhou, Y., Zhou, T., Zhang, Z., Liang, Z., Liang, W., Wang, A., et al. (2017). Characteristics and Formation Mechanism of Soft-Sediment Deformation Structures Related to Volcanic Earthquakes of the Lower Cretaceous Qingshan Group in Lingshan Island, Shandong Province. *JPOC* 19 (4), 567–582. doi:10.7605/gdlxb.2017.04.044

Conflict of Interest: The authors declare that the research was conducted in the absence of any commercial or financial relationships that could be construed as a potential conflict of interest.

Publisher's Note: All claims expressed in this article are solely those of the authors and do not necessarily represent those of their affiliated organizations, or those of the publisher, the editors, and the reviewers. Any product that may be evaluated in this article, or claim that may be made by its manufacturer, is not guaranteed or endorsed by the publisher.